J Med Allied Sci 2012; 2 (2): 41-48
www.jmas.in
Print ISSN: 2231 1696 Online ISSN: 2231 170X
Journal of Medical & Allied Sciences

Review

Raman based imaging in biological application- a perspective

Partha P. Kundu and Chandrabhas Narayana

Light Scattering Laboratory, Chemistry and Physics of Materials Unit,
Jawaharlal Nehru Center for Advanced Scientific Research, Jakkur, Bengaluru-560064, Karnataka, India.

Article history

Received 16 April 2012
Revised 08 June 2012
Accepted 19 July 2012
Early online 25 July 2012
Print 31 August 2012

Corresponding author

Chandrabhas Narayana

Professor,
Chemistry and Physics of Materials Unit,
Jawaharlal Nehru Centre for Advanced Scientific Research,
Jakkur P.O., Bengaluru-560064,
Karnataka, India.
Phone: +91 80 22082810
Fax: +91 80 22082766
Email: cbhas@jncasr.ac.in

Abstract

Imaging by means of Raman spectroscopy has emerged as a powerful technique in the study of various chemical processes occurring in biology. This technique is non-invasive, label-free, capable of providing molecular identity and can be performed in robust conditions. However, one major drawback is its inherently weak signal. The ways to overcome this issue is to use Raman based methods e.g. Resonance Raman Spectroscopy (RRS), Surface Enhanced Raman Spectroscopy (SERS), Tip Enhanced Raman Spectroscopy (TERS). In this review, we gave a brief introduction of all these methods, with special emphasis on their recent advances and applications in various fields of life science.

Key words: Raman, Resonance Raman, SERS, TERS, imaging

Knowledge of the distribution of chemical components is crucial in biology for monitoring biochemical processes. The ultimate goal is to develop a tool which is highly sensitive, chemically specific and which brings about little or no damage to the sample. To date, the techniques that are used for this purpose are fluorescence spectroscopy, electron paramagnetic resonance spectroscopy (EPR)[1], nuclear magnetic resonance spectroscopy (NMR)[2], high frequency ultrasound[3], to name a few. But none of these meet all the criteria mentioned above. Of them fluorescence spectroscopy has been used widely, especially in *in-vivo* studies, which provides a spatial resolution of few tens of nanometers[4,5], but it requires label a to be attached which may change the physical properties of the sample under investigation. Raman spectroscopy can be an alternative tool which provides "fingerprint" of a molecule. It is a label-free technique that can be applied in liquid state, which is beneficial as a biological sample can be probed in a state similar to its natural environment.

Raman Spectroscopy

When a monochromatic light is incident on an analyte most of the light will be scattered elastically and have the same frequency as the incident one. Only a small fraction of the incident light will be inelastically scattered and will have either higher or lower frequency compared to the incident one. In a Raman experiment it is the difference which is measured, and this gives the information of various vibrational levels present in the analyte. Raman can provide detailed information of the chemical bond present which in turn gives its structural information. Not only can it provide its structural information, but also the knowledge of its environment (e.g. hydrogen bonding or any other intermolecular interactions). This is important as those interactions play a crucial role in biology.

In Raman imaging a pseudo-color image is generated where the color of each pixel represents the intensity of a particular band or range of bands. Since the band is a marker for a particular component it provides the distribution of the desired compound over the sample. For biological sample the Raman spectra obtained are complicated and interpretation of the data is not trivial; some statistical analysis (e.g. Hierarchical Cluster Analysis (HCA), Principal Component Analysis (PCA), and Linear Discriminant Analysis (LDA)) is required.

Meister et al. investigated the uptake and cellular distribution of water soluble, organometallic, carbonyl complex $[Mn(tpm)(CO)_3]Cl$, an antitumor compound, in a cancer cell by 3D Raman imaging[6]. They used C≡O bond stretching frequency as a marker to study how the compound is distributed over the cell with time. Guze et al.[7] could differentiate the normal and abnormal squamous cell carcinoma (SCC) in oral mucosa using micro-Raman spectroscopy. The molecular changes which occurred because of disease could be identified by acquiring the Raman image both in normal cell and SSC cell. Raman images with rich information about structural features within the cytoplasm, cell membrane and cell nuclei were obtained, and spectral differences between normal and malignant squamous cells could be recognized. They could find a biomarker peak, believed to be originating from cell surface protein, greatly upregulated in SSC cell. Huang and co-workers[8] monitored cell division, in vivo, of a single living *Schizosaccharomyces pombe* cell at the molecular level by Raman imaging with spatial resolution of 0.3 µm. By analyzing the modes within fingerprint region (800–1800 cm^{-1}) they found that both the concentration and distribution of the two major cellular components, phospholipids and proteins, change simultaneously during and after the division of the *pombe* cell.

Although it is a powerful technique in elucidating structural information, the challenge remains as this is a very weak process (only 1 photon out of about 10^6 -10^8 incidents are Raman scattered). One way of get out of this issue is to use Resonance technique. In resonance Raman, the frequency of the excitation laser used is chosen in such a way that it coincide with one of the excited state of the analyte, thus it can enhance the signal by a factor of 10^3-10^7. In resonance Raman only a fraction of vibrational modes are enhanced, thus by suitably choosing the laser wavelength one can enhance certain vibrations of biological interest. For biological sample it is preferable to use NIR (near infrared) laser compared to UV laser as the latter can produce fluorescence background making the Raman signal hard to detect. Also another advantage of using NIR is the large penetration depth inside the tissue and less damage to the sample.

Bonifacio et al.[9] applied resonance Raman spectroscopy (RRS) to probe the distribution of hemoglobin and hemozoin (formed by parasites) within the parasitized cells at the molecular level. The set of spectra was collected from human erythrocytes infected with the malaria parasite *Plasmodium falciparum* and analyzed by statistical algorithm. This study would help in understanding the mechanism of formation of hemozoin and its interaction with antimalarial drugs, facilitating design of new drugs. Neugebauer et al.[10] applied UV resonance Raman spectroscopy to study bacterial growth of a *Bacillus pumilus* batch culture. The excitation wavelength used specifically enhanced signal from aromatic amino acid residues and nucleic acid bases. At the beginning of the exponential growth phase a drug from the fluoroquinolone group was added to the bacterial suspension. Using multivariative analysis they could detect small changes in the spectra upon interaction of the drug with its targets—DNA and enzyme gyrase inside the cell. A diagnostic tool was proposed based on RRS by Wood et al[11]. A strong band at 1569 cm^{-1} was chosen as a marker for detection of hemozoin. With ultransensitive rapid read-out CCD detectable signal could be acquired in 1 second. After multivariate analysis of the image obtained it was possible to detect the presence of hemozoin, indicating the possibility to identify low-pigmented phases of the parasite's life cycle including early trophozoites**.**

As mentioned earlier, Raman process is very weak restricting its use in cases where sample concentration is very less. Increasing laser power may be helpful, but there is an upper limit upto which it can be increased. So some alternative method is required.

Surface Enhanced Raman Spectroscopy (SERS)

In 1974 Fleischmann et al.[12] first observed a drastic increase in intensity of Raman signal from few molecules at the interface of metal electrodes. Later Jeanmaire and Van Duyne[13] found that the Raman signal can be greatly enhanced when a molecule is adsorbed on a roughened noble metal surface. Although complete understanding of the mechanism of enhancement is yet to be achieved, it is accepted that there are two mechanisms responsible for this enhancement-electromagnetic[14] and chemical[15]. When light is incident on a metal nano-

particle or metal nanostructure, it induces collective motion of the free electrons present in metal. These motions, known as localized surface plasmon resonance (LSPR), may cause strong electromagnetic field to be generated near the nanostructure in the resonance condition, and responsible for the electromagnetic enhancement in SERS. Chemical contribution arises due to three reasons:

1. Chemical enhancement due to the chemical interaction of the molecule with nanoparticle
2. Resonance Raman enhancement due to the resonance of the exciting source with one of the electronic transition of the molecule
3. Charge-Transfer (CT) resonance enhancement due to the resonance of the laser frequency with the molecule-nanoparticle charge transfer transition.

The total enhancement factor is around 10^6-10^8 on an average which could be up to 10^{14}, if the molecule is in a junction of a few nanoparticles in high electric field known as "hot spot"[16]. It is to be noted that the enhancement factor decays as r^{-12}, r is the distance of the analyte from the nanoparticle surface[17]. So the major contribution in SERS signal originates from those parts which are within a few nanometers from the nanoparticle.

Large variety of SERS substrate are used ranging from island films, roughened electrodes, colloidal nanoparticle of which colloidal nanoparticle are commonly used for Raman imaging *in vivo*. The advantage of using the nanoparticle, is its small size compared to the cell size. Also it can be incorporated into the cell with minimal damage to the cell membrane and after incorporation to the cell component. Their incorporation into the cell and distribution inside the cell can be controlled by functionalizing them with biological ligands or antibodies[18]. After the discovery of the silver and gold sols used for SERS[19], it has become most popular in SERS study[20]. Fabrication of nanoparticle by chemical reduction is inexpensive and simple. A metal salt is reduced by chemical agent to produce colloidal solution. The nanoparticle thus formed as different size, ranging from 10-80 nm depending upon the method of preparation. The plasmon resonances of these nanoparticles occur at different positions depending upon the shape, size and dielectric constant of the metal.

SERS has been used to detect the cancer markers in live cells[21]. Oh et al. synthesized Au_{core}/Ag_{shell} bimetallic nanoparticle conjugated with anti-mouse IgG. Each nanoparticle is tagged with R6G as Raman marker. In order to differentiate between the cancer cell and normal cell, PLCγ1 were used as the optical imaging targets inside HEK293 (human embryonic kidney) cells. Their results showed that functionalized nanoparticles attached only with the marker of the cancer cells by antibody-antibody interaction. SERS image of Raman marker in the cancer cell where PLCγ1 was expressed could be obtained. Whereas in the normal cell, no SERS image from the marker R6G could be obtained. All the results were verified by Quantum Dot (QD) labeled fluorescence images (Fig. 1).

Ravindranath et al.[22] performed SERS imaging to look into the intracellular bioreduction pockets of toxic chromate in Shewanella. In their study they used intracellularly grown Ag nanoisland as SERS substrate to detect the cellular localization of Cr(VI) and Cr (III). Raman bands for Cr(VI) in the 815-875 cm^{-1} range and for Cr(III) at 510-535 cm^{-1} were found to be characteristic for these states. Single-cell mapping experiments were performed using a 6 x 6 μm^2 area with an image resolution of ~22.5 x103 nm^2. Both Cr(VI) and reduced Cr(III) were observed in cells grown under aerobic and anaerobic conditions, but control samples grown in the absence of Cr(VI) did not show either form of chromium within the cellular periphery (Fig. 2).

These results show the capability of SERS imaging to probe the multiple metal reduction reaction inside a single cell. Ando et al.[23] probed the time dependent local molecular information by dynamic SERS imaging. Here a gold nanoparticle is used as a SERS substrate which moves around the cell and provide enhanced Raman signal of cellular components. Simultaneously, the track of the particle was monitored by dark field microscope. Spectral features of protein and lipids could be found within time span of 150 S. The spatial resolution of the image is ~65 nm, which is much shorter than diffraction limit of the light (which limits the resolution with which an object can be imaged by optical microscopy) and temporal resolution of 50 ms (Fig. 3). This study opens up the possibility of studying biological events using SERS imaging.

Tip Enhanced Raman Spectroscopy (TERS)

In studying biological samples it is desired to have a probe with high sensitivity and high lateral resolution to investigate the non-uniformity of various components to get insight into the system. Although SERS can fulfill the first criterion, its use in biology is limited by its poor resolution (~1µm). Also SERS substrate suffers from the fact that they are non-uniform in shape/size resulting in different enhancement to the Raman signal. Wessel[24] first proposed the concept of TERS based on optical-

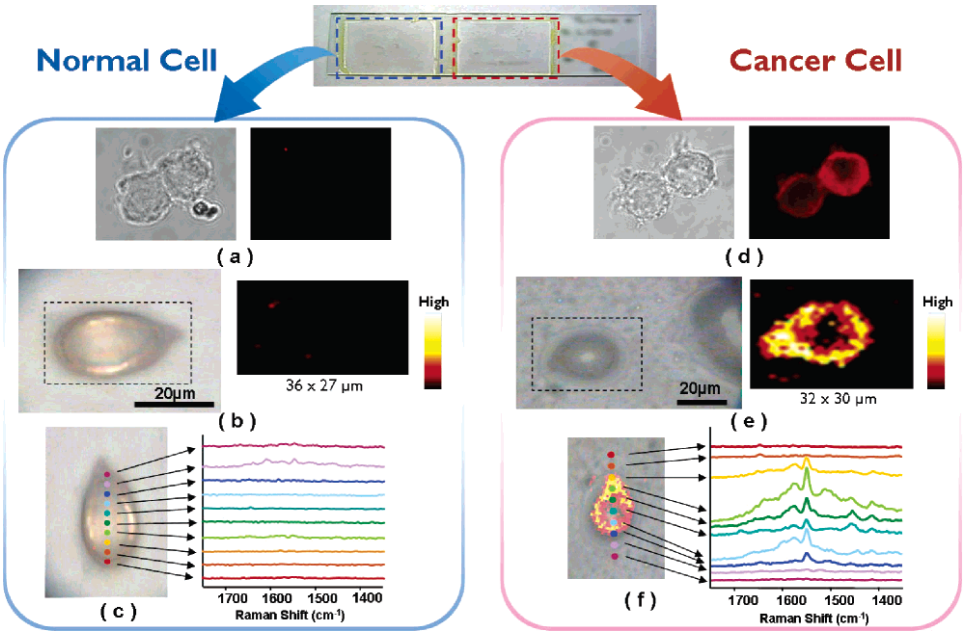

Fig 1. Fluorescence and SERS images of normal HEK293 cells and PLCγ1-expressing HEK293 cells. (a) Quantum Dot-labeled fluorescence images of normal cells: (left) brightfield image, (right) fluorescence image. (b) SERS images of single normal cell: (left) brightfield image, (right) Raman mapping image of single normal cell based on the 1650-cm^{-1} R6G peak. (c) Overlay image of brightfield and Raman mapping for single normal cell. (d) QD-labeled fluorescence images of cancer cells: (left) brightfield image, (right) fluorescence image. (e) SERS images of single cancer cell: (left) brightfield image, (right) Raman mapping image of single cancer cell based on the 1650-cm^{-1} R6G peak. (f) Overlay image of brightfield and Raman mapping for single cancer cell. (Adapted with permission from ref. 21. Copyright (2007) American Chemical Society)

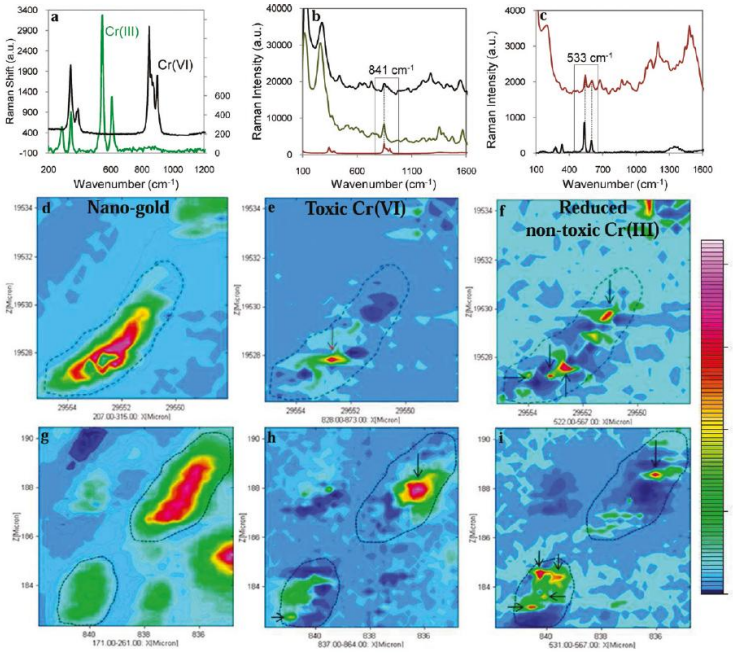

Fig 2. (a) Raman signatures for chemical control of Cr(VI) and Cr(III) show differences in their chemical spectra. (b) SERS spectra point to the presence of Cr(VI) peaks within the cells .The peaks from the chemical control (red) at 841 cm^{-1} align with the Cr(VI) peaks detected from within the cell. (c) Bacterial SERS spectrum (red) indicates the presence of Cr(III) peaks, aligned with those of the chemical control, Cr(III) (black spectrum). The two peaks of Cr(III) present around 533 cm^{-1} are perfectly aligned with the intracellularly reduced Cr(III). Raman intensity maps (aerobic reduction, d-f; anaerobic reduction, g-i) averaged over the phonon-plasmon peak (~230 cm^{-1}) showing the presence of intracellular pockets of gold nanoislands (d and g), localization of toxic hexavalent chromium, Cr(VI) (e and h), and reduced nontoxic chromium, Cr(III) (f and i), within a single cell. (Adapted with permission from ref. 22. Copyright (2011) American Chemical Society)

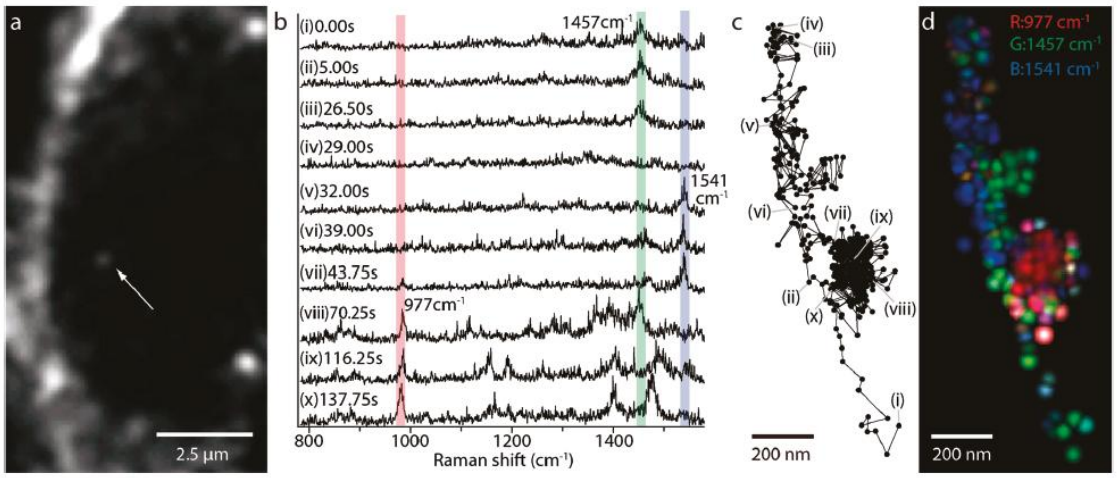

Fig 3. (a) An image of a macrophage cell taken by dark-field microscope. (b) SERS spectra, obtained from the nanoparticle indicated in panel-(a). (c) Trajectory of the nanoparticle, shown by a white arrow in panel-(a), (d) An RGB color map of the molecular distribution presented on the nanoparticle trajectory. Green spots show the Raman intensity distribution of 1457 cm^{-1}, blue spots 1541 cm^{-1}, and red spots 977 cm^{-1}. The green and blue color is highlighted during the linear paths, while the red color appears during the confined zone random walk. (Adapted with permission from ref. 23. Copyright (2011) American Chemical Society)

field confinement and enhancement by surface plasmon originating from metal nanoparticle. It has been shown theoretically by controlling the size of the nanoparticle one can achieve spatial resolution down to molecular level with 1nm tip apex radius. In a typical TERS set up a plasmonic metal nanoparticle or a sharp metallic edge is placed at the point of a tip. A scanning probe microscope scans the sample keeping the tip at a fixed position. Two types of scanning probes are used, scanning tunneling microscope (STM)[25] and atomic force microscope (AFM)[26]. In STM based TERS set up, etched silver or gold wire is used as a probe, while in AFM single particle is mounted at the tip by evaporation or sputtering of silver or gold. Although silver provide better enhancement than gold, it is prone to oxidation losing its enhancing power. STM is limited by the fact that only conducting sample or thin layer of non-conducting sample on a conducting substrate can be scanned, therefore use of AFM is more general. In AFM scanning is done either in contact or non-contact mode, for biological sample non-contact mode is preferable to avoid any damage. A typical TERS setup is shown in figure 4. A laser is illuminating the tip and the sample. Enhanced signal from the sample in the presence of tip is collected by a microscope objective. For biological sample, in order to prevent it from being damaged, the laser power is kept low (< 1mW). Typical wavelength used in for laser is 500-800nm. Initially AFM tip provides the morphology of the sample. Then depending upon the problem of interest, enhanced Raman image is acquired on selected points or small area providing molecular fingerprinting. Since the enhanced electric field produced is confined very close to the apex of the tip, only those molecules underneath it will be enhanced providing resolution in the nanometer range. It is to be noted that in TERS experiment information of sample is only extracted from the surface, if information from deep inside is required, section has to be done. Enhancement attained by TERS ranges from 10^4-10^6.

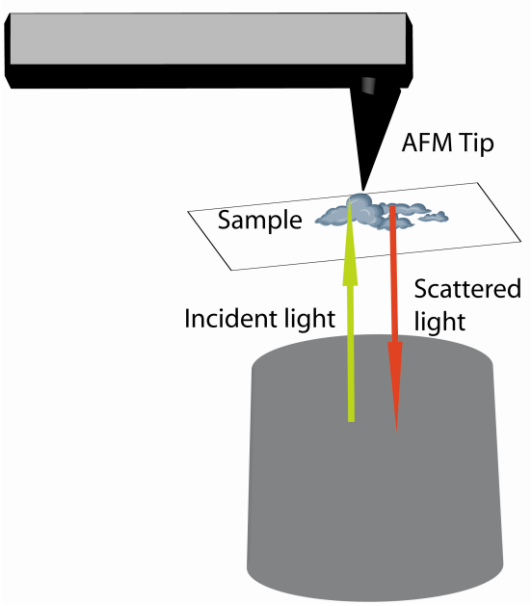

Fig 4. A typical tip enhanced Raman scattering setup

Enhancement mechanism in TERS is similar to that of SERS. When laser is irradiated on the apex of the tip surface plasmon will be generated there. If the peak of surface plasmon coincides with the wavelength of the laser, strong electromagnetic

field is generated at the apex of the tip, and its magnitude depends upon refractive index of the sample substrate, the tip material and its geometry. It has been shown[27] that materials with low refractive indices such as SiN, SiO_x and AlF_3 perform better compared to Si with high refractive index. The intensity can also be increased by placing the sample on a gold substrate, named as gap-mode[28]. Since intensity is square of the electric field the enhancement in intensity due to the tip also is squared. Tip itself acts like an antenna which creates its own electric field under the influence of the enhanced electric field. So the intensity of electromagnetic field is again enhanced by a power of two. So an overall enhancement of power of four is achieved. This is the electromagnetic contribution of the enhancement. Another enhancement can occur due to 'lightning rod' effect. Tip is illuminated in such a way; polarization of incident wave is along the tip apex, causing accumulation of electron density to increase at sharp edge. This cause both increase in field strength and confinement of field. There is also a possibility of chemical enhancement. When the tip is in direct contact with the sample, charge transfer can occur. This causes chemical enhancement associated with shift in band position[29].

The cell wall of *Staphylococcus epidermidis* was probed by TERS by Neugebauer et al.[30]. Contribution of TERS bands was mainly from N-acetyl glucosamine (NAG), a constituent of the biopolymer cell surface. Spectral fluctuation was observed, which was explained as capturing dynamic process occurring on the cell surface. However, this could be due to change in orientation of the molecule near tip. Recently, Richter et al.[31] reported for the first time TERS mapping of the distribution of protein and lipid on the membrane of human colon-cancer cell. The cell was fixed with formalin which was shown to cause minimal change to the integrity of the cell. For detection of protein amide bands were chosen as a marker while for lipid detection PO_2, CH_2, CH_3 vibrations were used. All the data was analyzed by multivariate technique. Wood et al.[32] performed TERS combined with AFM on sectioned cell for the first time. At first the AFM image of *Plasmodium falciparum*-infected erythrocytes were constructed to identify hemozoin crystal deposits and then selectively Raman spectra were recorded at a resolution ca. 10 nm from the edges of those deposits (Fig. 5). Spectra obtained from these crystals showed that they were in five-coordinate high-spin ferric state. This work would help to develop a label-free technique to detect hemozoin drug binding without isolating the hemozoin crystals. All these experiments described, were performed on fixed cell. Recently Schmid et al.[33] performed TERS in liquid state for the first time where both the tip and sample was immersed in water. The AFM tip coated with SiO_x/Ag was protected from the contamination by encapsulating a self-assembled monolayer. This study would help to perform TERS of biological samples in liquid state.

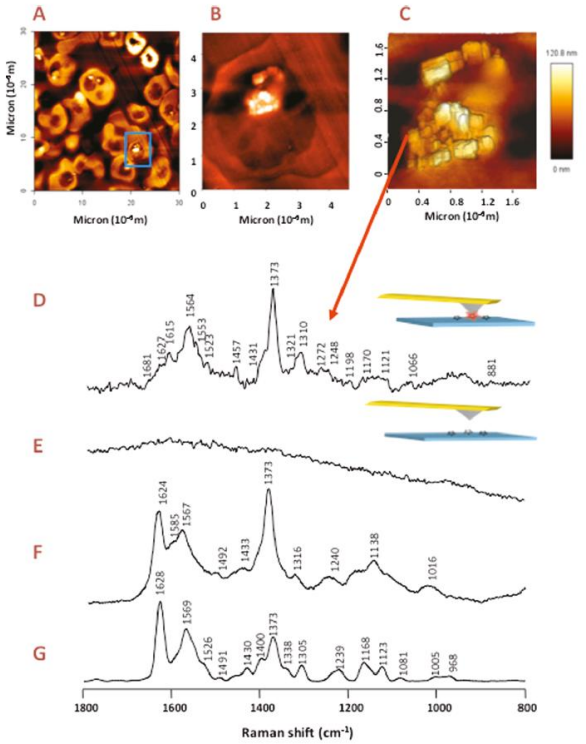

Fig 5. (A-C) AFM images recorded of sectioned cells before TERS acquisition. **(A)** A 30 X 30 µm AFM image recorded of a population of infected red blood cells. A potential cell target is highlighted by the blue square. **(B)** A high-resolution image of the cell highlighted in **(A)** depicting hemozoin crystals aligned in the digestive vacuole. **(C)** A higher resolution AFM image of the digestive vacuole of the parasite illustrating single crystals of hemozoin **(D)** TERS spectrum recorded of the edge of a hemozoin crystal. (E) Spectrum taken after retracting the tip to show that contamination does not happen at the tip. **(F)** SERS recorded of β-hematin prepared using SERS active Ag-particles. **(G)** Resonance Raman spectrum of β-hematin. (Adapted with permission from ref. 32. Copyright (2011) American Chemical Society)

Conclusion

Raman spectroscopy provides chemical information at molecular level in a non-invasive way. With the improvement in instrumentation, availability of database for various bio-molecules, use of multivariate technique to analyze complex data, Raman spectroscopy has become ideal bio-analytical tool. One of the major challenges is its intrinsic weak signal. Resonance Raman can increase the signal

by 10^4-10^7 times and making it possible to study sample at very low concentration if molecule of interest is a Raman active. Discovery of SERS made it possible to increase the signal up to 10^{14} times, providing study of even a single molecule. But it suffers from the non-reproducible spectra because of irregular enhancement of Raman signal. Since in TERS enhancing object is a single tip apex, enhancement is more regular and quantitative analysis is possible to some extent. Also one unique feature of TERS is its ability to provide label-free chemical information at nano scale level, which is beyond the reach of any other technique. Moreover, it is not restricted for liquid sample, so possibility of studying biological samples *in-vivo* is feasible. We believe that with the advent of new technology and multidisciplinary research, Raman and its associated techniques will be able to address many unsolved problems in biology.

Acknowledgments

Partha P. Kundu would like to thank CSIR, India for senior research fellowship. Authors are thankful to the copyright holders for giving us permission to reproduce figures.

Conflict of interest: None

References

1. Savitsky A and Möbius K. High-field EPR. Photosynth Res 2009; 102(2-3):311-333.
2. Li D, Keresztes I, Hopson R, Williard PG. Characterization of reactive intermediates by multinuclear diffusion-ordered NMR spectroscopy (DOSY). Acc Chem Res 2008; 42(2):270-280.
3. Budde RP, Bakker PF, Gründeman PF, Borst C. High-frequency epicardial ultrasound: review of a multipurpose intraoperative tool for coronary surgery. Surg Endosc 2009; 23(3):467-476.
4. Patterson G, Davidson M, Manley S, Lippincott-Schwartz J. Superresolution Imaging using single-molecule localization. Annu Rev Phys Chem 2010; 61(1): 345-367.
5. Schermelleh L, Heintzmann R, Leonhardt H. A guide to super-resolution fluorescence microscopy. J Cell Biol 2010; 190(2):165-175.
6. Meister K, Niesel J, Schatzschneider U, Metzler-Nolte N, Schmidt D, Havenith M. Label-free imaging of metal-carbonyl complexes in live cells by Raman microspectroscopy. Angew Chem Int Ed Engl 2010; 49(19):3310-3312.
7. Guze K, Short M, Zeng H, Lerman M, Sonis S. Comparison of molecular images as defined by Raman spectra between normal mucosa and squamous cell carcinoma in the oral cavity. J Raman Spectrosc 2011; 42(6):1232-1239.
8. Huang CK, Hamaguchi H, Shigeto S. In vivo multimode Raman imaging reveals concerted molecular composition and distribution changes during yeast cell cycle. Chem Commun 2011; 47(33):9423-9425.
9. Bonifacio A, Finaurini S, Krafft C, Parapini S, Taramelli D, Sergo V. Spatial distribution of heme species in erythrocytes infected with Plasmodium falciparum by use of resonance Raman imaging and multivariate analysis. Anal Bioanal Chem 2008; 392(7):1277-1282.
10. Neugebauer U, Schmid U, Baumann K, Holzgrabe U, Ziebuhr W, Kozitskaya S, Kiefer W, Schmitt M, Popp J. Characterization of bacterial growth and the influence of antibiotics by means of UV resonance Raman spectroscopy. Biopolymers 2006; 82(4):306-311.
11. Wood BR, Hermelink A, Lasch P, Bambery KR, Webster GT, Khiavi MA, Cooke BM, Deed S, Naumann D, McNaughton D. Resonance Raman microscopy in combination with partial dark-field microscopy lights up a new path in malaria diagnostics. Analyst 2009; 134(6):1119-1125.
12. Fleischmann M, Hendra PJ, McQuillan AJ. Raman spectra of pyridine adsorbed at a silver electrode. Chem Phys Lett 1974; 26(2):163-166.
13. Jeanmaire DL and Van Duyne RP. Surface Raman spectroelectrochemistry: Part I. Heterocyclic, aromatic, and aliphatic amines adsorbed on the anodized silver electrode. J Electroanal Chem 1977; 84(1): 1-20.
14. Qin L, Zou S, Xue C, Atkinson A, Schatz GC, Mirkin CA. Designing, fabricating, and imaging Raman hot spots. Proc Natl Acad Sci U S A 2006; 103(36):13300-13303.
15. Otto A. What is observed in single molecule SERS, and why? J Raman Spectrosc 2002; 33(8):593-598.
16. Kneipp K, Wang Y, Kneipp H, Itzkan I, Dasari RR, Feld MS. Population pumping of excited vibrational states by spontaneous surface-enhanced Raman scattering. Phys Rev Lett 1996; 76(14):2444-2447.
17. Kneipp K, Kneipp H, Itzkan I, Dasari RR, Feld MS. Surface-enhanced Raman scattering and biophysics. J Phys Condens Mat 2002; 14(18):R597-624.
18. Qian X, Peng XH, Ansari DO, Yin-Goen Q, Chen GZ, Shin DM, Yang L. Young AN, Wang MD, Nie S. In vivo tumor targeting and spectroscopic detection with surface-enhanced Raman nanoparticle tags. Nat Biotech 2008; 26(1):83-90.
19. Creighton JA, Blatchford CG, Albrecht MG. Plasma resonance enhancement of Raman scattering by pyridine adsorbed on silver or gold sol particles of size comparable to the excitation wavelength. J Chem Soc, Faraday Trans. 2 1979; 75:790-798.
20. Aroca RF, Alvarez-Puebla RA, Pieczonka N, Sanchez-Cortez S, Garcia-Ramos JV. Surface-enhanced Raman scattering on colloidal nanostructures. Adv Colloid Interface Sci 2005; 116(1-3):45-61.
21. Lee S, Kim S, Choo J, Shin SY, Lee YH, Choi HY, Ha S, Kang K, Oh CH. Biological imaging of HEK293 cells expressing PLCγ1 using surface-enhanced Raman microscopy. Anal Chem 2007; 79(3):916-922.
22. Ravindranath SP, Henne KL, Thompson DK, Irudayaraj J. Raman chemical imaging of chromate reduction sites in a single bacterium using intracellularly grown gold nanoislands. ACS Nano 2011; 5(6):4729-4736.
23. Ando J, Fujita K, Smith NI, Kawata S. Dynamic SERS imaging of cellular transport pathways with endocytosed gold nanoparticles. Nano Lett 2011; 11(12):5344-5348.
24. Wessel J. Surface-enhanced optical microscopy. J Opt Soc Am B 1985; 2(9):1538-1541.
25. Binnig G, Rohrer H, Gerber C, Weibel E. Surface studies

by scanning tunneling microscopy. Phys Rev Lett 1982; 49(1):57-61.
26. Binnig G, Quate CF, Gerber C. Atomic force microscope. Phys Rev Lett 1986: 56(9):930-933.
27. Yeo BS, Schmid T, Zhang W, Zenobi R. Towards rapid nanoscale chemical analysis using tip-enhanced Raman spectroscopy with Ag-coated dielectric tips. Anal Bioanal Chem 2007; 387(8):2655-2662.
28. Ikeda K, Fujimoto N, Uehara H, Uosaki K. Raman scattering of aryl isocyanide monolayers on atomically flat Au(1 1 1) single crystal surfaces enhanced by gap-mode plasmon excitation. Chem Phys Lett 2008; 460(1-3):205-208.
29. Lombardi JR, Birke RL, Lu T, Xu J. Charge-transfer theory of surface enhanced Raman spectroscopy: Herzberg--Teller contributions. J Chem Phys 1986; 84(8):4174-4180.
30. Neugebauer U, Schmid U, Baumann K, Ziebuhr W, Kozitskaya S, Deckert V, Schmitt M, Popp J. Towards a detailed understanding of bacterial metabolism—spectroscopic characterization of Staphylococcus epidermidis. Chem Phys Chem 2007; 8(1):124-137.
31. Richter M, Hedegaard M, Deckert-Gaudig T, Lampen P, Deckert V. Laterally resolved and direct spectroscopic evidence of nanometer-sized lipid and protein domains on a single cell. Small 2011; 7(2):209-214.
32. Wood BR, Bailo E, Khiavi MA, Tilley L, Deed S, Deckert-Gaudig T, McNaughton D, Deckert V. Tip-Enhanced Raman Scattering (TERS) from Hemozoin Crystals within a Sectioned Erythrocyte. Nano Lett 2011; 11 (5):1868-1873.
33. Schmid T, Yeo BS, Leong G, Stadler J, Zenobi R. Performing tip-enhanced Raman spectroscopy in liquids. J Raman Spectrosc 2009; 40(10):1392-1399.